

# Level Structure of $^{141}\text{Ba}$ and $^{139}\text{Xe}$ and the Level Systematics of $\text{N}=85$ Even-odd Isotones

Y.X. Luo<sup>1,2,3</sup>), J.O. Rasmussen<sup>4</sup>), J.H. Hamilton<sup>1</sup>), A.V. Ramayya<sup>1</sup>), J.K. Hwang<sup>1</sup>), C.J. Beyer<sup>1</sup>), S.J. Zhu<sup>3,5</sup>), J. Kormicki<sup>1</sup>), X.Q. Zhang<sup>1</sup>), E.F. Jones<sup>1</sup>), P.M. Gore<sup>1</sup>), T.N. Ginter<sup>4</sup>), K.E. Gregorich<sup>4</sup>), I-Yang Lee<sup>4</sup>), A.O. Macchiavelli<sup>4</sup>), P. Zielinski<sup>4</sup>), C.M. Folden III<sup>4</sup>), P. Fallon<sup>4</sup>), G.M. Ter-Akopian<sup>6</sup>), Yu.Ts. Oganessian<sup>6</sup>), A.V. Daniel<sup>6</sup>), M.A. Stoyer<sup>7</sup>), J.D. Cole<sup>8</sup>), R. Donangelo<sup>9</sup>), S.C. Wu<sup>10</sup>), and S.J. Asztalos<sup>11</sup>)

<sup>1</sup>) *Physics Department, Vanderbilt University, Nashville, TN 37235, USA*

<sup>2</sup>) *Institute of Modern Physics, CAS, Lanzhou, China*

<sup>3</sup>) *Joint Institute for Heavy Ion Research, Oak Ridge, TN 37830, USA*

<sup>4</sup>) *Lawrence Berkeley National Laboratory, Berkeley, CA 94720 USA*

<sup>5</sup>) *Physics Department, Tsinghua University,  
Beijing 100084, People's Rep. China*

<sup>6</sup>) *Flerov Laboratory for Nuclear Reactions, JINR, Dubna, Russia*

<sup>7</sup>) *Lawrence Livermore National Laboratory, Livermore, CA 94550, USA*

<sup>8</sup>) *Idaho National Environmental and Engineering Laboratory, Idaho Falls, ID 83415, USA*

<sup>9</sup>) *Universidade Federal do Rio de Janeiro, CP 68528, RG Brazil*

<sup>10</sup>) *Department of Physics, National Tsing Hua University, Hsinchu, Taiwan*

<sup>11</sup>) *Massachusetts Inst. of Technology, Cambridge, MA 11830, USA*

(Dated: January 31, 2002)

## Abstract

New level schemes of  $^{141}\text{Ba}$  and  $^{139}\text{Xe}$  are proposed from the analyses of spontaneous-fission gamma data from our  $^{252}\text{Cf}$  spontaneous fission Gammasphere runs of 1995 and 2000. By analogy with the  $N = 85$  even-odd isotones  $^{149}\text{Gd}$ ,  $^{147}\text{Sm}$ , and  $^{145}\text{Nd}$ , spins and parities were assigned to the observed excited states in  $^{141}\text{Ba}$  and  $^{139}\text{Xe}$ . It appears that spherical shell model neutron excitations plus octupole phonons are an appropriate basis at the lower end of the bands. Going to higher spins it is clear that the soft rotor involving valence protons as well as neutrons becomes increasingly important in the configurations. Level systematics in the  $N = 85$  even-odd isotones from  $\text{Gd}(Z=64)$  through  $\text{Te}(Z=52)$ , are discussed. The excitation systematics and smooth trends of the analogous levels support the spin and parity assignments for excited levels observed in  $^{141}\text{Ba}$  and  $^{139}\text{Xe}$ . The level systematics and the comparison with neighboring even-even isotopes indicate that quadrupole and octupole collectivity play roles in  $^{141}\text{Ba}$  and  $^{139}\text{Xe}$ . From  $\text{Gd}(Z=64)$  through  $\text{Te}(Z=52)$ , increasing excitation energies of the  $13/2^+$  states and lowering relative intensities of the positive parity bands in the  $N = 85$  even-odd isotones may indicate that the octupole strength is becoming weaker for the isotones when approaching the  $Z = 50$  closed shell.

PACS numbers: PACS number(s): 21.10.Re, 23.20.Lv, 27.60.+j, 27.70.+q

## I.

### Introduction

The  $N = 85$  even-odd nuclei are three neutrons beyond the 82-neutron closed shell. This intermediate region is too close to the closed shell for the simple strong-deformation model, yet far enough from doubly magic  $^{132}\text{Sn}$  to make shell model interpretations difficult. Showing extensive and complex band structure, these so-called 'quasi- $f_{7/2}$ ' nuclei provide a good opportunity to study the interplay between the single-particle excitations and the quasi-collective motions. The  $N = 85$  even-odd isotones are at the border of the predicted quadrupole-octupole correlation island centered at  $N = 88$ ,  $Z = 56$  [1]. Theoretical calculations indicate that octupole excitations may occur in  $^{141}_{56}\text{Ba}$  and  $^{139}_{54}\text{Xe}$  [2]. Because of the octupole strength deduced from the  $\nu f_{7/2}i_{13/2}$  transitions, octupole excitations and their trends are of great interest with regard to the structure of  $N = 85$  even-odd isotones.

Piiparinen *et al.* in 1981 reported high-spin shell model excitations in  $^{149}_{64}\text{Gd}$  through  $(\alpha, xn)$  reactions [3]. Spin and parity assignments for the excited states were made by means of gamma directional correlation from oriented nuclei (DCO) and linear polarization measurements. Levels of  $^{149}_{64}\text{Gd}$  were interpreted as shell model multiplets and multiplets coupled with octupole-phonon excitations, such as  $\nu(f_{7/2})^3$ ,  $\nu h_{9/2}(f_{7/2})^2$ ,  $\nu(f_{7/2})^3 \otimes 3^-$ ,  $\nu h_{9/2}(f_{7/2})^2 \otimes 3^-$ , and  $\nu(f_{7/2})^3 \otimes 3^- \otimes 3^-$ . Energies of the  $\nu(f_{7/2})^3$  states agree only moderately with those calculated by using empirical two-nucleon interactions taken from  $^{148}_{64}\text{Gd}$  [3]. Urban *et al.* in 1996 presented level schemes for  $^{145}_{60}\text{Nd}$  and  $^{147}_{62}\text{Sm}$ , based largely on their work using heavy-ion reactions [4]. As with  $^{149}_{64}\text{Gd}$ , the excited levels of  $^{145}_{60}\text{Nd}$  and  $^{147}_{62}\text{Sm}$  were assigned to the three valence neutron excitations in a spherical potential or with octupole vibrations coupled to them. The  $^{143}_{58}\text{Ce}$  nucleus has many excited levels known from beta decay studies of its parent  $^{143}\text{La}$  [5], but its band structure is not known. Our collaboration in 1997 published first results on level schemes of  $^{141}_{56}\text{Ba}$  and  $^{139}_{54}\text{Xe}$ , based on our 1995 fission data at Gammasphere [6]. When the present work was going on, the first report on  $^{137}_{52}\text{Te}$ , using the data from fission of  $^{248}\text{Cm}$  at Eurogam2 gamma detector array, was reported by Urban *et al.* [7]. No octupole excitations were found in  $^{137}_{52}\text{Te}$ , and the two negative-parity bands observed were interpreted as excitations of the three valence neutrons.

In the present work, using our triple coincidence  $^{252}\text{Cf}$  Gammasphere data of 2000, we restudied the level structures of  $^{141}_{56}\text{Ba}$  and  $^{139}_{54}\text{Xe}$  to complete the level systematics for  $N =$

85 even-odd isotones from  $Z = 64$  through  $Z = 52$ . We also present additional analyses on  $^{141}_{56}\text{Ba}$  and  $^{139}_{54}\text{Xe}$ , based on minimally compressed spectra from our triple-coincidence  $^{252}\text{Cf}$  Gammasphere data of 1995. Spin and parity assignments and configuration interpretations are made for the excited levels observed in  $^{141}_{56}\text{Ba}$  and  $^{139}_{54}\text{Xe}$ . Parity doublet bands with both  $s=+i$  and  $s=-i$  are observed in  $^{141}\text{Ba}$ . The level systematics and trends of level structure for  $N = 85$  even-odd isotones are also discussed.

## II. EXPERIMENT AND DATA ANALYSIS

It has been shown that the combination of a multi-gamma detection array with a fission source provides a powerful tool for the studies of the high-spin structure of neutron-rich nuclei [8]. In our year 2000 run the Gammasphere had 102 Compton-suppressed Ge detectors. A fission source of  $^{252}\text{Cf}$  with a strength of  $62 \mu\text{Ci}$ , sandwiched between two Fe foils ( $10 \text{ mg/cm}^2$ ) was mounted in a 7.6 cm-diameter polyethylene ball centered in the Gammasphere. More than  $5.7 \times 10^{11}$  triple and higher fold events were accumulated in about four weeks of counting.

The assignments of transitions to the nuclei  $^{141}\text{Ba}$  and  $^{139}\text{Xe}$  were justified by the simultaneous observations of the complementary fission partners and by careful cross-checks using double gating. Figure 1 shows a double-gated spectrum for  $^{141}\text{Ba}$  indicating one of the newly found bands, band (4), observed in  $^{141}\text{Ba}$ . It can be seen that the fission partners  $^{106,107,108}\text{Mo}$  are simultaneously observed in the spectrum. An effort was made to determine transition energies and relative intensities as accurately as possible. Energy calibration was derived from known, well-determined (usually from beta decay studies of individual fission fragments) energies of transitions in our own data set. These results are in good agreement with those determined from the separate calibration measurements with familiar standards. From residuals of the energy calibration fit, a systematic error of  $\pm 0.1 \text{ keV}$  is assigned. With the minimally compressed data, various double-gated spectra were examined with least-squares peak-fitting code of Radford's gf3 program, which determined transition energies and relative intensities with statistical standard deviations. Figure 2 shows a gated spectrum based on minimally compressed data of 1995, showing the better resolution of the minimally compressed data for the overlapped peaks. (Raw data for gamma energies are 16384 channels from 0 to 5 MeV; our minimally compressed data array created by A. Daniel

is 8192 channels over this range.) Tables I and II list the energies with standard deviations and relative intensities obtained from Radford's gf3 program for the assigned  $^{141}_{56}\text{Ba}$  and  $^{139}_{54}\text{Xe}$  transitions, respectively.

### III. RESULTS AND DISCUSSION

#### A. New level schemes of $^{141}\text{Ba}$ and $^{139}\text{Xe}$

Our collaboration, Zhu *et al.* [6], presented a level scheme with three bands in  $^{141}\text{Ba}$ . A new level scheme of  $^{141}\text{Ba}$  with five bands proposed in the present work is shown in Figure 3. Zhu *et al.* also reported a level scheme of  $^{139}\text{Xe}$ , which consisted of four bands [6]. Shown in Figure 4 is the new level scheme of  $^{139}\text{Xe}$  developed in the present work. The energy values given for the levels were derived from a program used by the compilers of the Nuclear Data Sheets. This program takes as input the transition energies and their standard deviations. It then generates the statistically best values for level energies. For the figures we have rounded all level energies and transition energies to the nearest 0.1 keV (our estimated systematic standard deviation.) Therefore, occasionally the difference of initial and final level energies does not quite equal the labeled transition energy. The spin-parity assignments are all tentative, as indicated by the parentheses about all but the ground state. However, the fact that the fission products are formed with an average of six or more units of angular momentum greatly simplifies the construction of bands and assignment of spins, because only yrast or near-yrast states are observed. We are further helped in the cases of this paper by the fact that the bands are interlaced with each other. Thus, spin and parity assignments are quite constrained, since only E2, M1, and E1 multipolarities are expected to compete. Ideally, one would like to have internal conversion coefficients (ICC) or directional gamma-gamma correlation measurements to confirm multipolarity assignments. Measurement of ICCs for prompt fission gamma radiation is not feasible due to complexity of the large mix of fission product activities. In a few cases where one low energy (<150 keV) and one high energy (>200 keV) transitions are present in a cascade, the ICC for the low energy transition has been extracted by comparing the  $\gamma$ -ray intensities [9]. The Eurogam collaboration has made a few angular correlation measurements [10]. In their case the fission fragments were stopped in a KCl salt pill, a diamagnetic medium in which the perturbing

magnetic or electric fields at the stopped fission nuclei should be small. In all our Berkeley Gammasphere experiments we have stopped in metallic stoppers that could leave large residual perturbing fields. We hope that some groups will come forward to greatly expand the work in angular correlations and test the tentative spin-parity assignments proposed here.

Band (1) of  $^{141}\text{Ba}$  of Zhu *et al.* is confirmed up to  $(19/2^-)$ . However, their 814.0 keV transition is not observed. Instead, we place an 835.4 keV and, tentatively, an 869.8 keV transition on the top of this band, extending the spin to  $(27/2^-)$ . Band (2) of  $^{141}\text{Ba}$  is extended up by the 733.3 keV transition, reaching  $(29/2^-)$ . A 577.2 keV transition is observed in between the 1187.3 and 610.1 keV levels, so the band (2) is found to build on the 48.5 keV  $(5/2^-)$  level. The interconnecting transitions between bands (1) and (2) are confirmed. The band (3) is extended to spin  $33/2^+$  by the observation of a 784.4 keV transition. The previously tentatively reported dashed 495 keV transition in band (3) is observed. A new connecting transition between the 2114.9 keV level of band (1) and the 1836.2 keV level of band (3) was observed at 278.7 keV. Of particular interest are the two new bands, (4) and (5), which are proposed for the first time in  $^{141}\text{Ba}$ . Band (4) is extended to 4303.7 keV  $(31/2^-)$  level with its intertwined transitions of 335.9, 261.1, 348.2, and tentatively 346.3 keV between bands (4) and (3). Band(4) seems to be a bifurcation of band(1), and it is not clear which set of stretched E2 cross-over transitions above the  $15/2^-$  is best characterized as the extension of band(1). There are no crossing transitions observed between band(4) and band(1) except for the intense decay-out transition of 870.1 keV found to de-excite the 2172.2 keV  $(19/2^-)$  bottom level of band (4) to feed into the 1302.0 keV  $(15/2^-)$  level of band (1). In addition, cross transitions of 452.5 and 452.3 keV were found between bands (4) and (2). So the new band (4) not only decays into bands (1) and (2), but also interconnects with band (3). Consisting of three transitions, the high lying new band (5) reaches the 4931.7 keV  $(35/2^+)$  level, which is the highest excitation energy of any positive parity band found in the  $N = 85$  even-odd isotones. Intertwined transitions of 614.7, 231.3, 318.1, 415.2, and 335.8 keV were observed between bands (2) and (5).

Bands (1), (2), and (3) of  $^{139}\text{Xe}$  reported by Zhu *et al.* [6] are confirmed and extended tentatively by one level in each band, reaching 4985 keV,  $35/2^-$ , 6091 keV,  $41/2^-$ , and 4411.8 keV,  $33/2^-$ , respectively; the former two reach the highest excitations observed in all the  $N = 85$  even-odd isotones. Similar to  $^{141}\text{Ba}$ , band (2) is found to be built on the

31.7 keV ( $5/2^-$ ) level by observation of a 525.2 keV transition. Band (5) is confirmed and extended by observation of a 682.3 keV transition. Two new possible band heads, (4) and (6), are identified. Each consists of only one level.

The three close-lying levels, which lie lowest in the level scheme of  $^{141}\text{Ba}$  and  $^{139}\text{Xe}$ , were established by several beta-decay studies from 1972 to 1984, as cited in The Table of Isotopes [5]. Their spins and parities are assigned as ( $3/2^-$ ), ( $5/2^-$ ), and ( $7/2^-$ ). They are interconnected by M1 and E2 transitions, establishing a common parity. This trio of lowest levels is a common feature of the  $N = 85$  even-odd nuclei, though the level order sometimes changes. Typically for the  $N = 85$  even-odd nuclei, there is a gap of 0.6 to 0.8 MeV above the close trio near the ground state before the onset of a large number of negative parity excited states, and the higher spin, near-yrast bands form a sequence of levels connected by E2 transitions with about the same spacing as the gap. Such a common feature is seen in  $^{141}\text{Ba}$  and  $^{139}\text{Xe}$ , and other  $N = 85$  even-odd isotones, although in  $^{149}\text{Gd}$ ,  $^{147}\text{Sm}$ , and  $^{145}\text{Nd}$  the bands are seen only to lower excitations and spins.

The assignments of spins and parities to the excited levels of  $^{141}\text{Ba}$  and  $^{139}\text{Xe}$  are based on the level systematics and analogies to the even-odd isotones  $^{149}\text{Gd}$ ,  $^{147}\text{Sm}$ , and  $^{145}\text{Nd}$ , where the assignments were made by means of DCO and linear polarization measurements and shell model calculations, or by analogies of level systematics and decay patterns [3,4,7]. The yrast bands (1) in  $^{141}\text{Ba}$  and  $^{139}\text{Xe}$  are found to be built on the ( $7/2^-$ ) level, and, as mentioned above, band (2) is built on the ( $5/2^-$ ) level. Keeping this in mind and by analogy to the corresponding levels of the bands of  $^{149}\text{Gd}$ ,  $^{147}\text{Sm}$ , and  $^{145}\text{Nd}$ , the bands (1) and (2) of  $^{141}\text{Ba}$  and  $^{139}\text{Xe}$  are assigned as negative parity bands, which consist of cross-over  $\Delta I=2$  E2 transitions and form signature partners. The excitation and decay pattern of the newly observed 2172.2 keV level of  $^{141}\text{Ba}$  is analogous to the 2704 keV and 2408 keV ( $19/2^-$ ) levels in  $^{147}\text{Sm}$  and  $^{145}\text{Nd}$ , respectively, which suggests a ( $19/2^-$ ) assignment to this new level and negative parity to band (4) of  $^{141}\text{Ba}$ , which consists of E2 cross-over transitions. Such a band was not well developed in  $^{147}\text{Sm}$  and  $^{145}\text{Nd}$  [4]. The assignment of spins and positive parity to bands (3) and (5) of  $^{141}\text{Ba}$  and to bands (3) and (4) of  $^{139}\text{Xe}$  are made also based on the excitation systematics and decay patterns similar to those of the other  $N = 85$  even-odd isotones. The positive parity bands (3) and (5) of  $^{141}\text{Ba}$  extend to the highest spins and excitation energies, 4618.6 keV ( $33/2^+$ ) and 4931.7 keV ( $35/2^+$ ), respectively, among all isotones studied. So parity doublets with both simplex quantum numbers  $s = +i$

(bands (1) and (3)) and  $s = -i$  (bands (2) and (5)) characteristics of octupole deformation are identified in  $^{141}\text{Ba}$ , as seen in  $^{149}\text{Gd}$ ,  $^{147}\text{Sm}$ , and  $^{145}\text{Nd}$ , although in the latter three isotopes only lower spins and excitations are observed to be populated. The two parity doublets in  $^{141}\text{Ba}$  are interconnected by E1 transitions. Note that some parity assignments differ from Zhu *et al.* [6]. In  $^{139}\text{Xe}$ , however, only one level of 3548.0 keV ( $27/2^+$ ) is assigned to the higher-lying positive parity band (4), so only the  $s = +i$  parity doublet, bands (1) and (3), is identified. The positive parity band (3) in  $^{139}\text{Xe}$  is pushed up to considerably higher excitation energies, starting from 1512.4 keV, and is very weakly populated (see Figure 4 and Table II). So between bands (1) and (2) there are only E1 transitions de-exciting the levels of band (3) and feeding those of band (1) in  $^{139}\text{Xe}$ . Moreover, the positive parity band (4) in  $^{139}\text{Xe}$  starts from the 3548.0 keV ( $27/2^+$ ) level, the highest level among all the  $N = 85$  even-odd isotones.

Table III lists the  $B(E1)/B(E2)$  ratios calculated for levels in  $^{141}\text{Ba}$  and the corresponding information for  $^{139}\text{Xe}$ . We suggest in the next section that it is difficult to draw conclusions about collectivity from these ratios, even if one has lifetime measurements, which have not been made for these levels.

### B. Interpretations for the excited levels of $^{141}\text{Ba}$ and $^{139}\text{Xe}$

The interpretations of the configurations for the excited levels of  $^{141}\text{Ba}$  and  $^{139}\text{Xe}$  are made based on the published decay studies as well as systematics and analogies to the other  $N = 85$  even-odd isotones. These earlier studies based on (Heavy ion, xn) reaction gamma work generally do not populate as high spins in the bands as does the spontaneous fission gamma work. Also, these studies were for  $Z=60$ , 62 and 64, all close to the 64 subshell with filled  $g_{7/2}$  and  $d_{5/2}$  proton orbitals. The earlier work mainly assigned configurations as excitations of the three valence neutrons, with proton participation entering only indirectly through octupole phonon couplings. We feel that this approach may be quite appropriate for the low end of the main bands, near the  $Z=64$  subshell, but we see no abrupt breaks in our  $Z=54$  and 56 bands when going above the maximum spins of stretched configurations of the three valence neutrons. Invoking double octupole excitations as in Refs. [3,4] seems to us questionable for our  $Z=54$  and 56 nuclei. Rather, we suggest that the participation of valence protons (four protons in  $^{139}\text{Xe}$  and six in  $^{141}\text{Ba}$ ) gradually increases as one goes up



the band to higher spins. The generally equal spacing of the bands is characteristic of soft rotors, as in a 3-dimensional harmonic oscillator.

The transition rates of the lowest-lying three levels in  $^{141}\text{Ba}$  and  $^{139}\text{Xe}$ , where measured, are slower than the single-proton formula, suggesting they are different couplings of the three valence neutrons, not much involving proton or collective shape phonons. The consensus is that these three levels represent different couplings of the three  $f_{7/2}$  neutrons,  $\nu(f_{7/2})^3$ . Couplings allowed by the Pauli principle are  $J = 3/2, 5/2, 7/2, 9/2, 11/2,$  and  $15/2$ . So  $\nu(f_{7/2})^3_{3/2}$ ,  $\nu(f_{7/2})^3_{5/2}$ , and  $\nu(f_{7/2})^3_{7/2}$  are assigned to the ground  $3/2^-$ , 48.5 keV ( $5/2^-$ ), and 55.0 keV ( $7/2^-$ ) levels of  $^{141}\text{Ba}$ , respectively, and the same configurations are assigned to the lowest levels in  $^{139}\text{Xe}$ . The configuration is probably dominant in lowest  $\nu(f_{7/2})^3$   $11/2^-$  and  $15/2^-$  levels of  $^{141}\text{Ba}$  and  $^{139}\text{Xe}$ . The beta decay studies suggested a  $\nu h_{9/2}$  single neutron excitations to the  $9/2^-$  level in  $^{149}\text{Gd}$  [11], excluding the  $\nu(f_{7/2})^3$  assignment, so  $\nu h_{9/2}(f_{7/2})^2$  was assigned to this  $9/2^-$  level in  $^{149}\text{Gd}$ , and also to the  $9/2^-$  state in  $^{147}\text{Sm}$  [12] and  $^{145}\text{Nd}$  [13] from single neutron transfer data. We assume their assignment is applicable also to our  $9/2^-$  states. However, the  $13/2^-$  state cannot be formed by  $\nu(f_{7/2})^3$ , so there is likely dominant  $\nu(f_{7/2})^2 h_{9/2}$  and some contributions from protons. Higher spin states in band(1) and (2) probably are a mixture of configurations involving  $f_{7/2}$  and  $h_{9/2}$  neutrons plus quadrupole phonons.

The  $13/2^+$  states in  $^{147}\text{Sm}$  and  $^{145}\text{Nd}$  were found to be populated with  $l = 6$  in single neutron transfer reactions, indicating the contribution to the  $13/2^+$  state by the  $\nu i_{13/2}$  single neutron excitations [ref. 4 and the papers referred to therein]. However, Piiparinen *et al.* [3] argued that the  $13/2^+$  is predominately due to octupole-phonon excitations coupled to the  $\nu(f_{7/2})^3$ , that is  $\nu(f_{7/2})^3 \otimes 3^-$ . The octupole phonon in this case is not the same as the core octupole phonon of  $^{132}\text{Sn}$  at 4.351 MeV, composed of nucleon particle hole states across the closed shells. In  $^{141}\text{Ba}$  the  $13/2^+$  state lies far lower at 1341 keV and in  $^{145}\text{Nd}$  at 1011 keV. The octupole phonon of Piiparinen *et al.* [3] must be composed mainly of valence-shell particle-hole excitations, mainly of the odd neutron, which can be promoted from  $f_{7/2}$  to  $i_{13/2}$  without the pair-breaking needed for proton excitations. Thus, there is not a clearcut choice between assignments of  $\nu(f_{7/2})^2 i_{13/2}$  and the  $\nu(f_{7/2})^3 \otimes 3^-$ .

In the  $Z=60$  ( $^{145}\text{Nd}$ ) isotone the ‘Octupole’ band has a bandhead of  $11/2^+$  close to the  $13/2^+$  and a doublet structure  $17/2^+$ ,  $15/2^+$  and  $21/2^+$ ,  $19/2^+$  above that. In our case of  $^{141}\text{Ba}$  the  $19/2^+$ ,  $15/2^+$  and  $11/2^+$  are not observed. The  $11/2^+$  state presumably arise from

a non-stretched ( $I_{stretch}-1$ ) coupling of  $f_{7/2}$  with the octupole phonon.

Band (4) of  $^{141}\text{Ba}$  is remarkable in that it is headed by a  $19/2^-$  level at 2172.2 keV remarkably close in energy (58 keV) to the level of the same spin and parity in band (1). The energy spacing in band (4) is also smaller than that in band (1), suggesting that band (4) has the greater deformation or quadrupole softness. One of two  $19/2^-$  levels in  $Z=60, 62$  and  $64$  isotones has been proposed as a double octupole-phonon state [3,4]. Such an explanation requires considerable anharmonicity of the octupole vibration to bring the state so low. A simpler explanation is that there are various reasonable configurations to make  $19/2^-$ , such as  $\pi(g_{7/2}^{-2})_2\nu(f_{7/2}^3)_{15/2}$ , or  $\nu(f_{7/2}^2)_6h_{9/2}$  etc..

The neat picture we might have hoped for would be a family of four interlaced bands, two of positive and two of negative parity. Then we could claim an example of both signature partner and parity doublet bands. However, the presence of five bands in  $^{141}\text{Ba}$  spoils the simple picture. Bands (1) - (4) of  $^{141}\text{Ba}$  are most tightly interlaced by transitions, while band (5) only seems interconnected with band (2). The lack of M1 transitions linking bands (3) and (5) argue against their being signature partners.

We believe it is premature to try to draw definite conclusions about octupole deformations from the  $B(E1)/B(E2)$  ratios of Table III. Even when lifetimes are known, the  $B(E1)$  strength is not a simple indicator of stable pear-shaped deformation. The E1 strength arises from a cross-term in the quadrupole and octupole transition matrix elements, which can give a separation of center-of-charge and center-of-mass during rotation or vibration. Any significant separation thus requires not only quadrupole and octupole collective motion, but also that the degree of participation of neutrons and protons be unequal. In cluster-model terms, E1 strength arises only when the charge-to-mass ratio of the core (such as  $^{132}\text{Sn}$ ) has a different  $Z/N$  ratio than the cluster beyond the core. What is clear is that there is both quadrupole and octupole collective strength in the  $N=85$  isotones.

### C. Level systematics of the $N = 85$ even-odd isotones

Now the systematics, analogies, and trends of the level patterns in  $N = 85$  even-odd isotones from Gd ( $Z = 64$ ) through Te ( $Z = 52$ ) are available and can provide important information on the nuclear structure for the isotones, including spin and parity assignments made for the excited levels observed in  $^{141}\text{Ba}$  and  $^{139}\text{Xe}$ .

Shown in Figure 5 are the level systematics of the two negative parity bands in the  $N = 85$  even-odd isotones, which, as discussed in the previous section, are interpreted in the spherical shell model as built on the 3-neutron ground states or excitations. Level systematics and smooth trends can be seen in Figure 5 from  ${}_{64}\text{Gd}$  through  ${}_{52}\text{Te}$  for the yrast negative parity band (band (1) in  ${}^{141}\text{Ba}$ , for example), and the yrast negative parity band (band (2) in  ${}^{141}\text{Ba}$ , and likely signature partner of band (1), for example). The positive parity state  $25/2^+$  has an almost constant energy as seen in Figure 6. It is of interest to note the evolution of the two bands with variation of proton number of the isotones. Moving down from Gd ( $Z = 64$ ), the irregularities of the two negative parity bands are decreasing, and around Ba ( $Z = 56$ ) the level spacing becomes more regular. This changing irregularity may be attributed to moving away from the strong  $Z = 64$  sub-shell. The comparative regularity observed in  ${}^{141}\text{Ba}$  and  ${}^{139}\text{Xe}$  may be an indication that quadrupole collectivity has come into play. The contributions of quadrupole collectivity to the nuclear structure of  ${}^{141}\text{Ba}$  and  ${}^{139}\text{Xe}$  are compared with those for their neighboring even-even isotopes  ${}^{140}\text{Ba}$  [16] and  ${}^{138}\text{Xe}$  [17] in Figure 7 and Figure 8, respectively, where the yrast levels of  ${}^{141}\text{Ba}$  and that of  ${}^{139}\text{Xe}$  are compared to those of  ${}^{140}\text{Ba}$  and  ${}^{138}\text{Xe}$ . It can be seen clearly that in comparison with  ${}^{140}\text{Ba}$  and  ${}^{138}\text{Xe}$ , respectively, the yrast bands of  ${}^{141}\text{Ba}$  and  ${}^{139}\text{Xe}$  are more regular and in fact more like a collective band.

Figure 6 depicts the systematics of lower-lying positive parity bands (band (3) in  ${}^{141}\text{Ba}$ , for example) in  $N = 85$  even-odd isotones, which is considered to build on the octupole phonon excitations coupled to  $\nu(f_{7/2})^3$ . Figure 9 is drawn for the higher-lying positive parity bands (band (5) in  ${}^{141}\text{Ba}$ , for example), which are accounted for by Urban *et al.* [4] as the octupole phonon excitations coupled to excited neutron configurations  $\nu h_{9/2}(f_{7/2})^2$  orbital. In Figure 6, of particular interest, is the variation of the excitation energies of the band heads of the lower-lying positive parity band,  $13/2^+$ , with changing proton number of the isotopes. It is more clearly seen in Figure 10 that with decreasing proton number the excitation energies of the  $13/2^+$  states are increasing, while those of the  $13/2^-$  states, band heads of the negative parity band (band (2) in  ${}^{141}\text{Ba}$ , for example), are decreasing in such a way that the  $13/2^+$  yrast state in Gd, Sm, and Nd becomes non-yrast in Ba and Xe isotones, and no  $13/2^+$  state is observed in the Te isotone. The pronounced trend of the excitation energies of the  $13/2^+$  state in the  $N = 85$  even-odd isotones may account for the decrease of relative intensities of the lower-lying positive parity band with decreasing proton number of the isotones, and

for the very weak population of the positive band (3) in  $^{139}\text{Xe}$  and the failure to observe a positive-parity band in  $^{137}\text{Te}$ . The rising excitation energies and the weakening population of the positive parity band with decreasing proton number of the isotones may imply that when approaching the  $Z = 50$  proton shell, the octupole excitations in the  $N = 85$  even-odd isotones become weaker.

#### IV. SUMMARY

New level schemes of  $^{141}\text{Ba}$  and  $^{139}\text{Xe}$  are proposed here up to an excitation of  $\approx 5$  MeV by using the triple- and higher-fold coincidence data from  $^{252}\text{Cf}$  spontaneous fission at Gammasphere obtained in year 2000, supplemented by minimally compressed spectra from our data of 1995. Spins and parities are proposed for the excited levels. Systematics of the yrast and near-yrast level structure of the  $N = 85$  even-odd isotones have been extended and expanded from  $Z = 64$  through  $Z = 52$ . Level systematics and analogies of decay patterns for the  $N = 85$  even-odd isotones support the spin and parity assignments. Lower-lying excited states in  $^{141}\text{Ba}$  and  $^{139}\text{Xe}$  are interpreted in the spherical shell model as valence neutron particle excitations, or as octupole excitations coupled with the single neutron states. However, quadrupole and octupole collectivity, showing up in the developed bands, limits the applications of the simple shell model in these nuclei and makes it likely that there is increasing participation of the valence protons in contributing angular momentum at higher spins. The level spacings of the observed bands in  $^{141}\text{Ba}$  and  $^{139}\text{Xe}$  become somewhat regular in comparison with those of isotones near  $Z = 64$  subshell, and this comparative regularity is seen when the yrast bands of  $^{141}\text{Ba}$  and  $^{139}\text{Xe}$  are compared to those of their neighboring even-even isotopes  $^{140}\text{Ba}$  and  $^{138}\text{Xe}$ , respectively. This suggests that the collective motions, primarily quadrupole rotation/vibrations, have come into play in  $^{141}\text{Ba}$  and  $^{139}\text{Xe}$ . The increasing excitation energies of the  $13/2^+$  states and the decreasing relative intensities of the positive parity bands of the  $N = 85$  even-odd isotones with decreasing proton number of the isotones may be an indication that when approaching the  $Z = 50$  proton shell, the octupole excitations of the  $N = 85$  even-odd isotones require more energy, and finally go above yrast and are not observable in the prompt fission gamma spectra.

#### ACKNOWLEDGMENTS

We wish to dedicate this paper to the memory of Dr. Stanley G. Thompson, who was

the leader in opening up the field of high-resolution spectroscopy of prompt-fission gamma rays nearly forty years ago. The work at Vanderbilt University, Lawrence Berkeley National Laboratory, Lawrence Livermore National Laboratory, and Idaho National Engineering and Environmental Laboratory are supported by U.S. Department of Energy under Grant No. DE-FG05-88ER40407 and Contract Nos. W-7405-ENG48, DE-AC03-76SF00098, and DE-AC07-76ID01570. The work at Tsinghua is supported by the National Natural Science Foundation and the Science Foundation for Nuclear Industry, China. The Joint Institute for Heavy Ion Research is supported by its members, U. of Tennessee, Vanderbilt, and the U.S. DOE through contract No. DE-FG05-87ER40311 with U. of Tennessee. The authors are indebted for the use of  $^{252}\text{Cf}$  to the office of Basic Energy Sciences, U.S. Department of Energy, through the transplutonium element production facilities at the Oak Ridge National Laboratory. The authors would also like to acknowledge the essential help of I. Ahmad, J. Greene and R.V.F. Janssens in preparing and lending the  $^{252}\text{Cf}$  source we used in the year 2000 runs.

- 
- [1] W. Nazarewicz and P. Olanders, Nucl. Phys. **A441** (3), 420 (1985).
  - [2] R.K. Sheline et al., Phys. Rev. **C38**(6), 2952 (1988).
  - [3] M. Piiparinen et al., Z. Phys. **A300**, 133 (1981).
  - [4] W. Urban et al., Phys. Rev. **C53**, 2516 (1996).
  - [5] R.B. Firestone and V.S. Shirley, eds., Table of Isotopes, Eighth Edition, 1996.
  - [6] S.J. Zhu et al., J. Phys. **G23**, Nucl. Part. Phys., L77 (1997).
  - [7] W. Urban et al., Phys. Rev. **C61**, 041301 (2000).
  - [8] J.H. Hamilton et al., Prog. Part. Nucl. Phys **35**, 635 (1995).
  - [9] J.K. Hwang et al., Phys. Rev **C56**, 1344 (1997).
  - [10] W. Urban et al., Nucl. Inst. and Meth. **A365**, 596 (1995).
  - [11] K.S. Toth et al., Phys. Rev. **C11**, 1370 (1975).
  - [12] J.B. Rekstad et al., Nucl. Phys. **A348**, 93 (1980).
  - [13] G. Lovhoiden et al., Nucl. Phys. **A339**, 477 (1980).
  - [14] B. Fornal et al., Phys. Rev. **C63**, 024322 (2001).
  - [15] Y. X. Luo et al., Phys. Rev **C64**, 054306 (2001).

- [16] S.J. Zhu et al., Chin. Phys. Lett. **14**, No. 8, 569 (1997).
- [17] A. Korgul et al., Eur. Phys. J. **A7**, 167 (2000).
- [18] Zs. Podolyak et al., Eur. Phys. J. **A8**, 147 (2000).
- [19] W. Urban et al., Phys. Lett. **B258**, 293 (1991).
- [20] W. Urban et al., Nucl.Phys. **A613**, 107 (1997).
- [21] A. Nowak et al., Eur. Phys. J. **A3**, 111 (1998).
- [22] P.D. Cottle et al., Phys. Rev. **C40**, 2028 (1989).
- [23] L. Bargioni et al., Phys. Rev. **C51**, R1057 (1995).

TABLE I: Transition energies, statistical standard deviations, and intensities in  $^{141}\text{Ba}$ 

$E_\gamma$ (keV)	$\sigma$ (keV)	$E_\gamma$ [6](keV)	Relative $I_\gamma$	Band	$I_i^\pi \rightarrow I_f^\pi$
588.59	0.02	588.9	100	1	$(11/2^-) \rightarrow (7/2^-)$
658.42	0.02	658.0	62.0	1	$(15/2^-) \rightarrow (11/2^-)$
812.94	0.05	812.9	11.5	1	$(19/2^-) \rightarrow (15/2^-)$
835.44	0.13		2.8	1	$(23/2^-) \rightarrow (19/2^-)$
869.8	0.4			1	$(27/2^-) \rightarrow (23/2^-)$
561.63	0.09	560.9	18	2	$(9/2^-) \rightarrow (5/2^-)$
577.26	0.09		3	2	$(13/2^-) \rightarrow (9/2^-)$
532.34	0.14	532.3	23	2	$(17/2^-) \rightarrow (13/2^-)$
609.49	0.07	609.3	17	2	$(21/2^-) \rightarrow (17/2^-)$
845.97	0.09	846.5	7.4	2	$(25/2^-) \rightarrow (21/2^-)$
733.34	0.15		1.4	2	$(29/2^-) \rightarrow (25/2^-)$
495.17	0.15	495	1.6	3	$(17/2^+) \rightarrow (13/2^+)$
596.96	0.14	596.6	12	3	$(21/2^+) \rightarrow (17/2^+)$
694.53	0.06	694.4	7	3	$(25/2^+) \rightarrow (21/2^+)$
706.42	0.09	706.3	5	3	$(29/2^+) \rightarrow (25/2^+)$
784.43	0.14		1.5	3	$(33/2^+) \rightarrow (29/2^+)$
609.28	0.11		6.2	4	$(23/2^-) \rightarrow (19/2^-)$
690.66	0.17		3.5	4	$(27/2^-) \rightarrow (23/2^-)$
831.5	0.12		1.1	4	$(31/2^-) \rightarrow (27/2^-)$
549.44	0.08		2.5	5	$(27/2^+) \rightarrow (23/2^+)$
751.04	0.11		1.6	5	$(31/2^+) \rightarrow (27/2^+)$
687.43	0.14		0.9	5	$(35/2^+) \rightarrow (31/2^+)$
555.14	0.11	554.5	12	2-1	$(9/2^-) \rightarrow (7/2^-)$
543.72	0.04	543.4	26	2-1	$(13/2^-) \rightarrow (11/2^-)$
417.58	0.04	417.9	22	2-1	$(17/2^-) \rightarrow (15/2^-)$
395.17	0.22	394.9	0.6	1-2	$(19/2^-) \rightarrow (17/2^-)$
214.26	0.26	214.0	1.0	2-1	$(21/2^-) \rightarrow (19/2^-)$
697.54	0.24	697.6	3	3-1	$(13/2^+) \rightarrow (11/2^-)$
534.22	0.08	534.3	15	3-1	$(17/2^+) \rightarrow (15/2^-)$
278.79	0.17		1.4	1-3	$(19/2^-) \rightarrow (17/2^+)$
318.34	0.06	317.9	4.2	3-1	$(21/2^+) \rightarrow (19/2^-)$
870.14	0.08		6.6	4-1	$(19/2^-) \rightarrow (15/2^-)$
452.5	0.1		3.9	4-2	$(19/2^-) \rightarrow (17/2^-)$
452.2	0.3			4-2	$(23/2^-) \rightarrow (21/2^-)$
335.96	0.16		2.8	4-3	$(19/2^-) \rightarrow (17/2^+)$
261.08	0.16		1.2	3-4	$(21/2^+) \rightarrow (19/2^-)$
348.44	0.22			4-3	$(23/2^-) \rightarrow (21/2^+)$
614.66	0.05		3.2	5-2	$(23/2^+) \rightarrow (21/2^-)$
231.42	0.14		0.6	2-5	$(25/2^-) \rightarrow (23/2^+)$
318.14	0.09		3.4	5-2	$(27/2^+) \rightarrow (25/2^-)$
415.2	0.2			2-5	$(29/2^-) \rightarrow (27/2^+)$
335.64	0.22		0.8	5-2	$(31/2^+) \rightarrow (29/2^-)$

## Figure captions

**Figure 1.** Double-gated spectrum on 870.1 and 658.4 keV transitions in  $^{141}\text{Ba}$ , using the triple-coincidence  $^{252}\text{Cf}$  fission data from Gammasphere of 2000 run. The new band (4) in  $^{141}\text{Ba}$ , consisting of 609.3, 690.7, and 831.5 keV transitions and the interconnecting transition of 261.1 keV, is identified, and the transitions of its fission partners are simultaneously seen.

**Figure 2.** Double-gated spectrum on 571.1keV ( $11/2^- \rightarrow 7/2^-$ ) and 581.7 keV ( $21/2^- \rightarrow 17/2^-$ ) in  $^{139}\text{Xe}$ , using triple-coincidence with minimally compressed (16k to 8k) data array. The cascade through the intermediate  $13/2^-$ -level generates two transitions of nearly equal energies, so close that they are unresolvable with the compression necessary in our Radware cube. This figure shows the non-linear least-squares fit using Radford's ft2 function in the spectral analysis program gf3 for the complex peak  $\sim 491$  keV and ft1 for the clean peak  $\approx 585.3$  keV. The data and individual and summed peaks are shown, as well as the linear background and the residual errors in the fit. Peak widths were fixed by a formula based on fitting clean peaks, so in the 2-peak fit there were 6 variables, two for the linear background, two peak positions, and two peak heights. The placement of 490.9- and 491.8-keV in the level scheme is fixed by energy sums of alternate paths, and the energy sums agree within 0.1 keV.

**Figure 3.** New level scheme of  $^{141}\text{Ba}$  established in the present work. See text.

**Figure 4.** New level scheme of  $^{139}\text{Xe}$  established in the present work. See text.

**Figure 5.** Level systematics of the two negative parity bands of the  $N = 85$  even-odd isotones, which are interpreted in the spherical shell model basis on single neutron excitations. Also shown in the figure are systematics for the  $25/2^+$  state, which is interpreted as pure neutron excitations. The  $19/2^-$  states are interpreted by Piiparinen *et al.* [3] and Urban *et al.* [4] as double-phonon excitations coupled with single neutron states. See text for our alternative interpretations.

**Figure 6.** Level systematics of the lower-lying positive parity bands of the  $N = 85$  even-odd isotones, which are interpreted to build on octupole phonon excitations coupled with single neutron ground states. For the sake of completeness for the bands, the  $25/2^+$  member of the bands is also shown in the figure.

**Figure 7.** Comparison of the yrast band of  $^{141}\text{Ba}$  with that of the neighboring even-even isotope  $^{140}\text{Ba}$  (data taken from [16]). Also shown in the figure is the comparison for



the octupole phonon band in  $^{140}\text{Ba}$  and the positive parity band in  $^{141}\text{Ba}$ , the latter is interpreted as octupole phonon excitations coupled with single neutron excitations.

**Figure 8.** Comparison of the yrast band of  $^{139}\text{Xe}$  with that of the neighboring even-even isotope  $^{138}\text{Xe}$  (data taken from [17]).

**Figure 9.** Level systematics of the higher-lying positive parity band of the  $N=85$  even-odd isotones. This has been interpreted in ref. 4 as an octupole phonon excitation coupled with single-particle neutron states with one neutron promoted from the  $f_{7/2}$  to the  $h_{9/2}$  orbital. Note that in Te isotones there is no positive parity band observed.

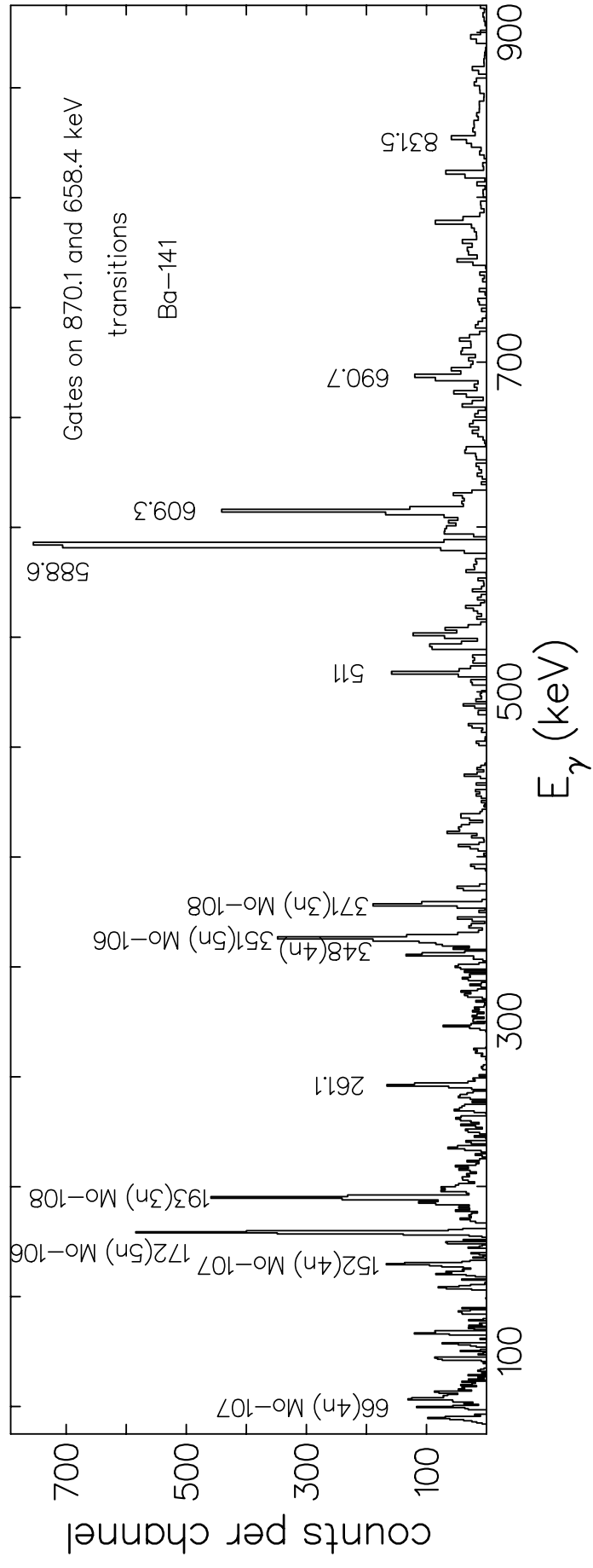
**Figure 10.** Trends of the excitation energies of the band head,  $13/2^+$ , of the lower-lying positive parity bands of the  $N = 85$  even-odd isotones. Also shown in the figure are the  $13/2^-$  states. The  $13/2^+$  is rising in excitation energy when proton number is decreasing, becoming non-yrast for Ba and Xe isotones. Also shown in the figure are the energy differences between the  $3^-$  states of the  $N = 84$  even-even isotones and the  $13/2^+$  states of the neighboring  $N = 85$  even-odd isotones. The data of  $N = 84$  isotones are taken from [16] and [18-23]. Also see text.

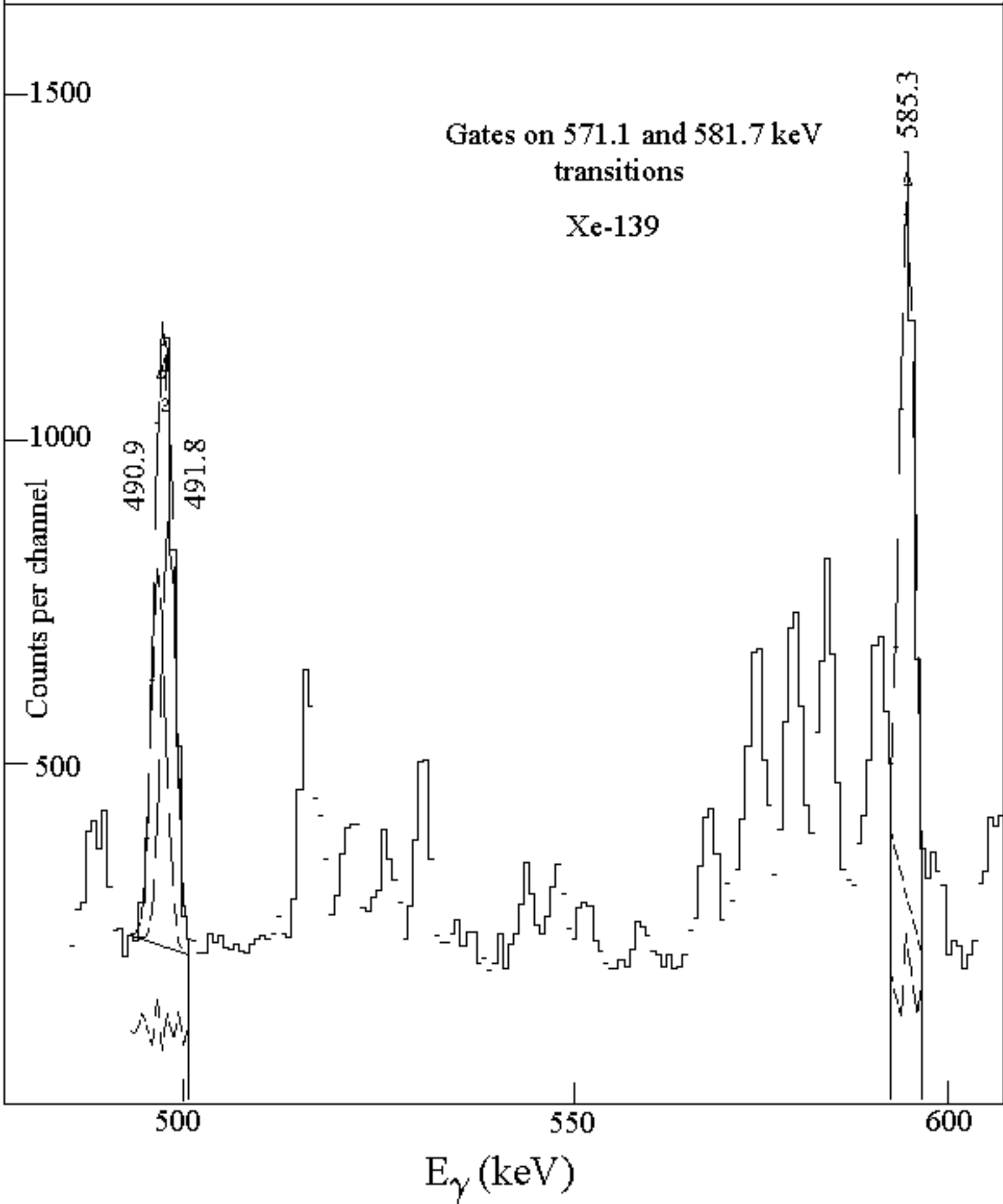
TABLE II: Transition energies, statistical standard deviations, and intensities in  $^{139}\text{Xe}$ 

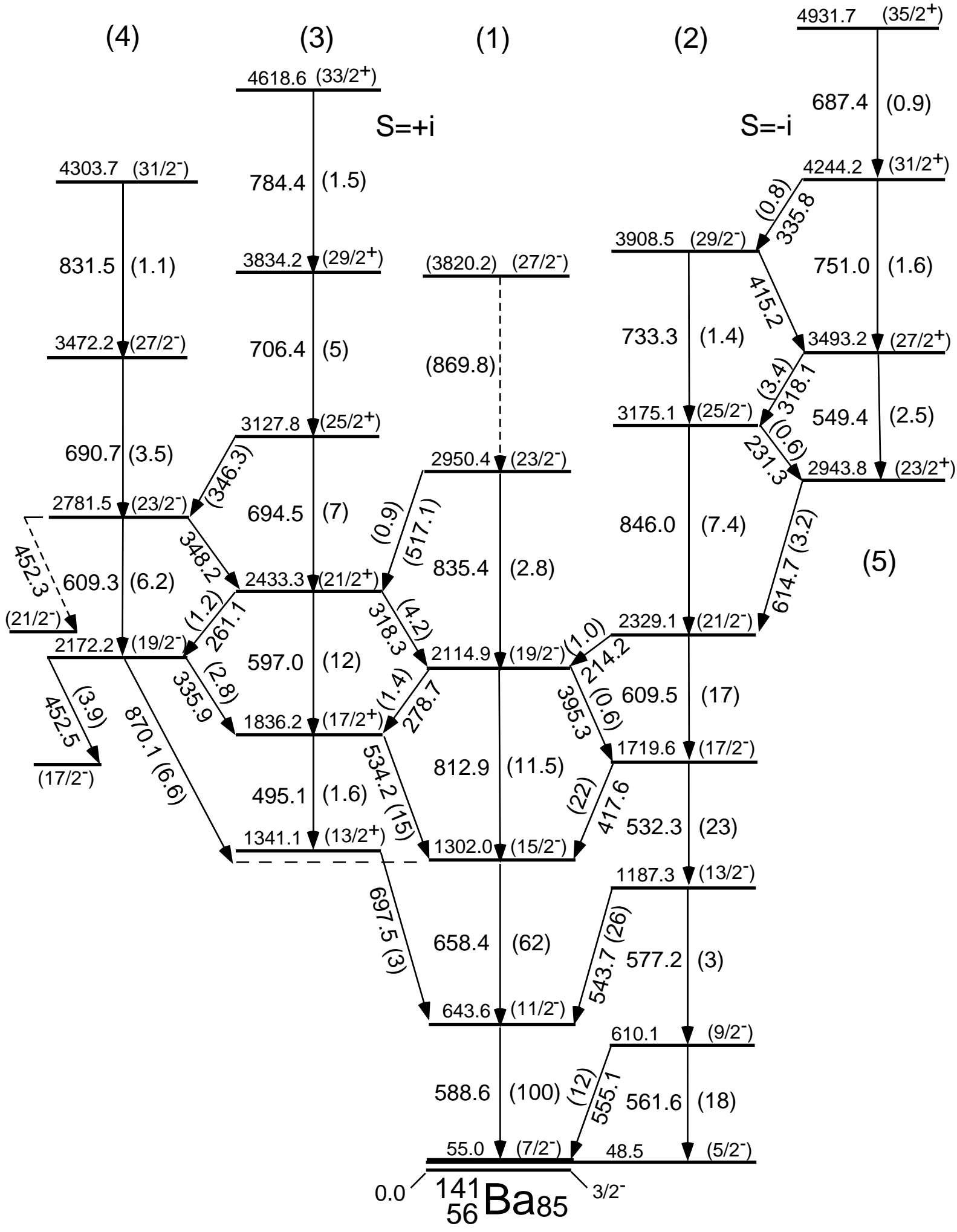
$E_\gamma$ (keV)	$\sigma$ (keV)	$E_\gamma$ [6](keV)	Relative $I_\gamma$	Band	$I_i^\pi \rightarrow I_f^\pi$
571.11	0.02	571.4	100	1	$(11/2^-) \rightarrow (7/2^-)$
585.32	0.03	585.2	71	1	$(15/2^-) \rightarrow (11/2^-)$
630.38	0.03	630.5	22	1	$(19/2^-) \rightarrow (15/2^-)$
690.24	0.09	690.5	8	1	$(23/2^-) \rightarrow (19/2^-)$
661.52	0.07	661.7	3.3	1	$(27/2^-) \rightarrow (23/2^-)$
861.49	0.15	861.9	1	1	$(31/2^-) \rightarrow (27/2^-)$
962	0.4			1	$(35/2^-) \rightarrow (31/2^-)$
527.92	0.09	528.1	12	2	$(9/2^-) \rightarrow (5/2^-)$
525.24	0.09		3	2	$(13/2^-) \rightarrow (9/2^-)$
491.77	0.09	491		2	$(17/2^-) \rightarrow (13/2^-)$
581.74	0.07	582.3	18	2	$(21/2^-) \rightarrow (17/2^-)$
763.03	0.09	763.3	7.9	2	$(25/2^-) \rightarrow (21/2^-)$
664.16	0.09	664.2	4.3	2	$(29/2^-) \rightarrow (25/2^-)$
646.53	0.08	646.7	1.4	2	$(33/2^-) \rightarrow (29/2^-)$
863.94	0.09	864.3	1.2	2	$(37/2^-) \rightarrow (33/2^-)$
995	0.4			2	$(41/2^-) \rightarrow (37/2^-)$
502.02	0.2	502.6	0.4	3	$(17/2^+) \rightarrow (13/2^+)$
560.27	0.14	560.7	1.1	3	$(21/2^+) \rightarrow (17/2^+)$
636.65	0.15	636.2	2.6	3	$(25/2^+) \rightarrow (21/2^+)$
580.94	0.15	580.8	0.8	3	$(29/2^+) \rightarrow (25/2^+)$
619.63	0.11			3	$(33/2^+) \rightarrow (29/2^+)$
732.74	0.16	732.5	1.8	5	
682.3	0.24		0.9	5	
918.54	0.12	918.3	2	3-1	$(13/2^+) \rightarrow (11/2^-)$
835.14	0.09	835.4	4.9	3-1	$(17/2^+) \rightarrow (15/2^-)$
765.04	0.19	765.6	2.2	3-1	$(21/2^+) \rightarrow (19/2^-)$
711.34	0.11	711.7	1.7	3-1	$(25/2^+) \rightarrow (23/2^-)$
536.94	0.09	537.2	9	2-1	$(9/2^-) \rightarrow (7/2^-)$
490.88	0.09	492		2-1	$(13/2^-) \rightarrow (11/2^-)$
397.53	0.05	397.4	17	2-1	$(17/2^-) \rightarrow (15/2^-)$
232.78	0.18	233.1	2	1-2	$(19/2^-) \rightarrow (17/2^-)$
348.98	0.2	349.2	2.5	2-1	$(21/2^-) \rightarrow (19/2^-)$
341.3	0.3	341.3	1.5	1-2	$(23/2^-) \rightarrow (21/2^-)$
1013.4	0.4	1013.2	1.6	5-1	
382.67	0.12	383.0	1.2	5-1	
1115.7	0.3	1115.7	0.8	5-1	
425.1	0.3	425		5-1	
805.04	0.2		1.7	6-1	
626.52	0.12		1.6	4-2	$(27/2^+) \rightarrow (25/2^-)$

TABLE III: Experimental  $B(E1)/B(E2)$  ratios in  $^{141}\text{Ba}$  and  $^{139}\text{Xe}$ 

	$E_\gamma$ (keV)	$I_i^\pi \rightarrow I_f^\pi$	$B(E1)/B(E2)(10^{-6}\text{fm}^{-2})$
$^{141}\text{Ba}$ , s = +i	812.9	$(19/2^-) \rightarrow (15/2^-)$	1.54(8)
Bands (1)	278.7	$(19/2^-) \rightarrow (17/2^+)$	
and (3)	835.4	$(23/2^-) \rightarrow (19/2^-)$	0.73(6)
	517.1	$(23/2^-) \rightarrow (21/2^+)$	
	495.1	$(17/2^+) \rightarrow (13/2^+)$	1.41(8)
	534.2	$(17/2^+) \rightarrow (15/2^-)$	
	597.0	$(21/2^+) \rightarrow (17/2^+)$	0.63(5)
	318.3	$(21/2^+) \rightarrow (19/2^-)$	
Bands (3)	597.0	$(21/2^+) \rightarrow (17/2^+)$	0.33(4)
and (4)	261.1	$(21/2^+) \rightarrow (19/2^-)$	
$^{141}\text{Ba}$ , s = -i	846.0	$(25/2^-) \rightarrow (21/2^-)$	2.18(9)
Bands (2)	231.3	$(25/2^-) \rightarrow (23/2^+)$	
and (5)	549.4	$(27/2^+) \rightarrow (23/2^+)$	1.63(8)
	318.1	$(27/2^+) \rightarrow (25/2^-)$	
	751.0	$(31/2^+) \rightarrow (27/2^+)$	2.43(9)
	335.8	$(31/2^+) \rightarrow (29/2^-)$	
$^{139}\text{Xe}$ , s = +i	501.9	$(17/2^+) \rightarrow (13/2^+)$	0.52(5)
Bands (1)	835.1	$(17/2^+) \rightarrow (15/2^-)$	
and (3)	560.3	$(21/2^+) \rightarrow (17/2^+)$	0.19(3)
	765.0	$(21/2^+) \rightarrow (19/2^-)$	
	636.6	$(25/2^+) \rightarrow (21/2^+)$	0.15(5)
	711.4	$(25/2^+) \rightarrow (23/2^-)$	







(3)

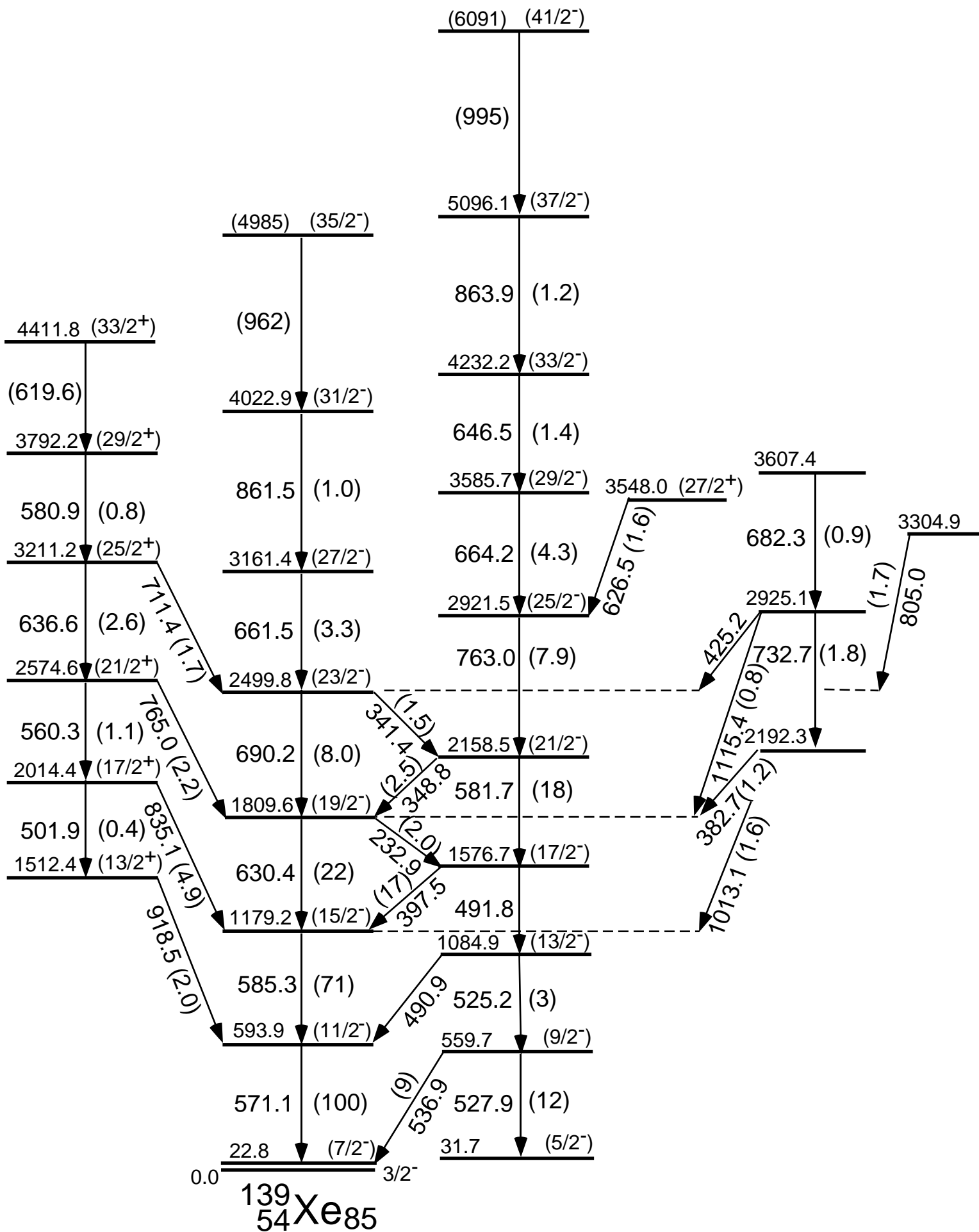
(1)

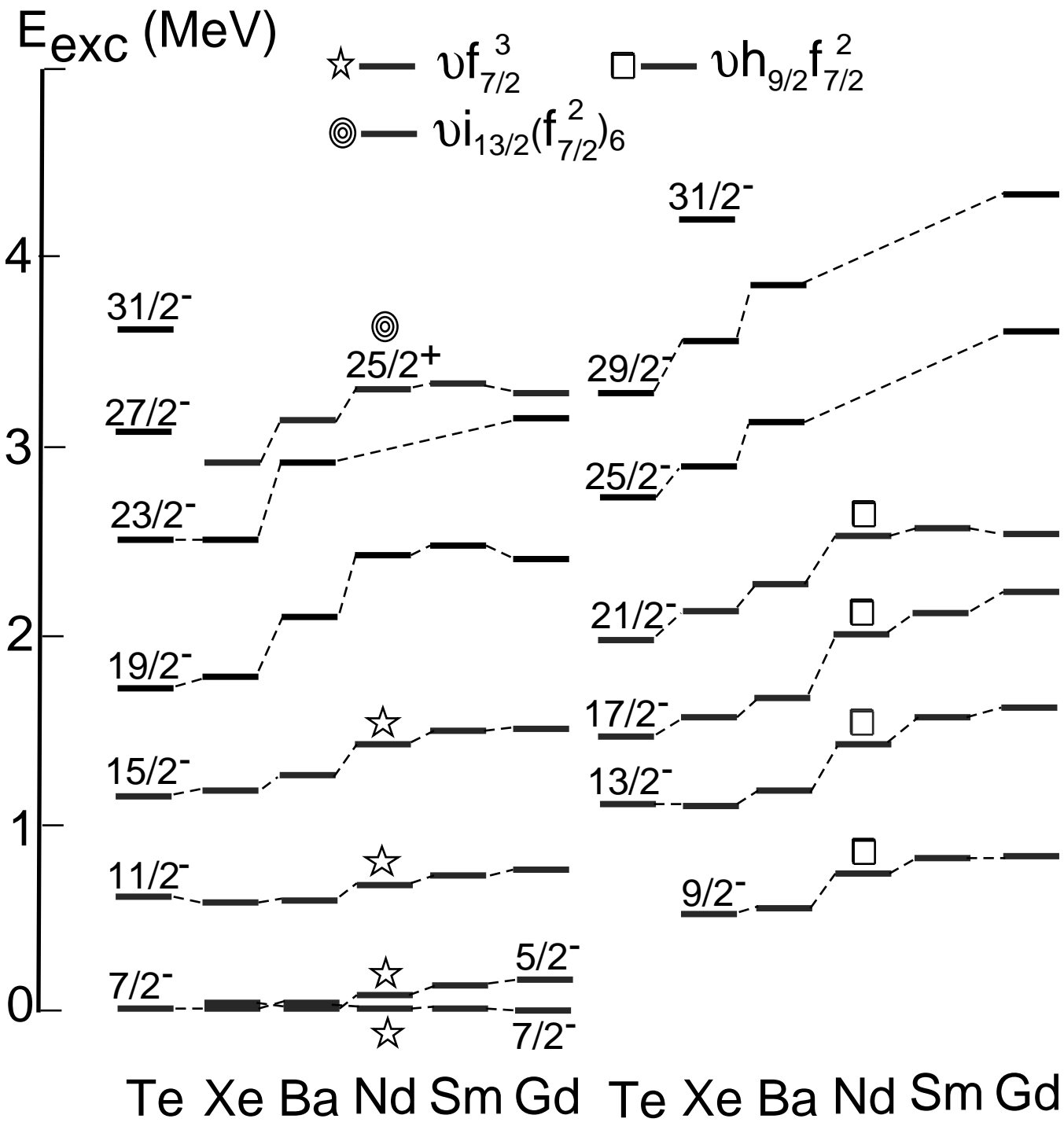
(2)

(4)

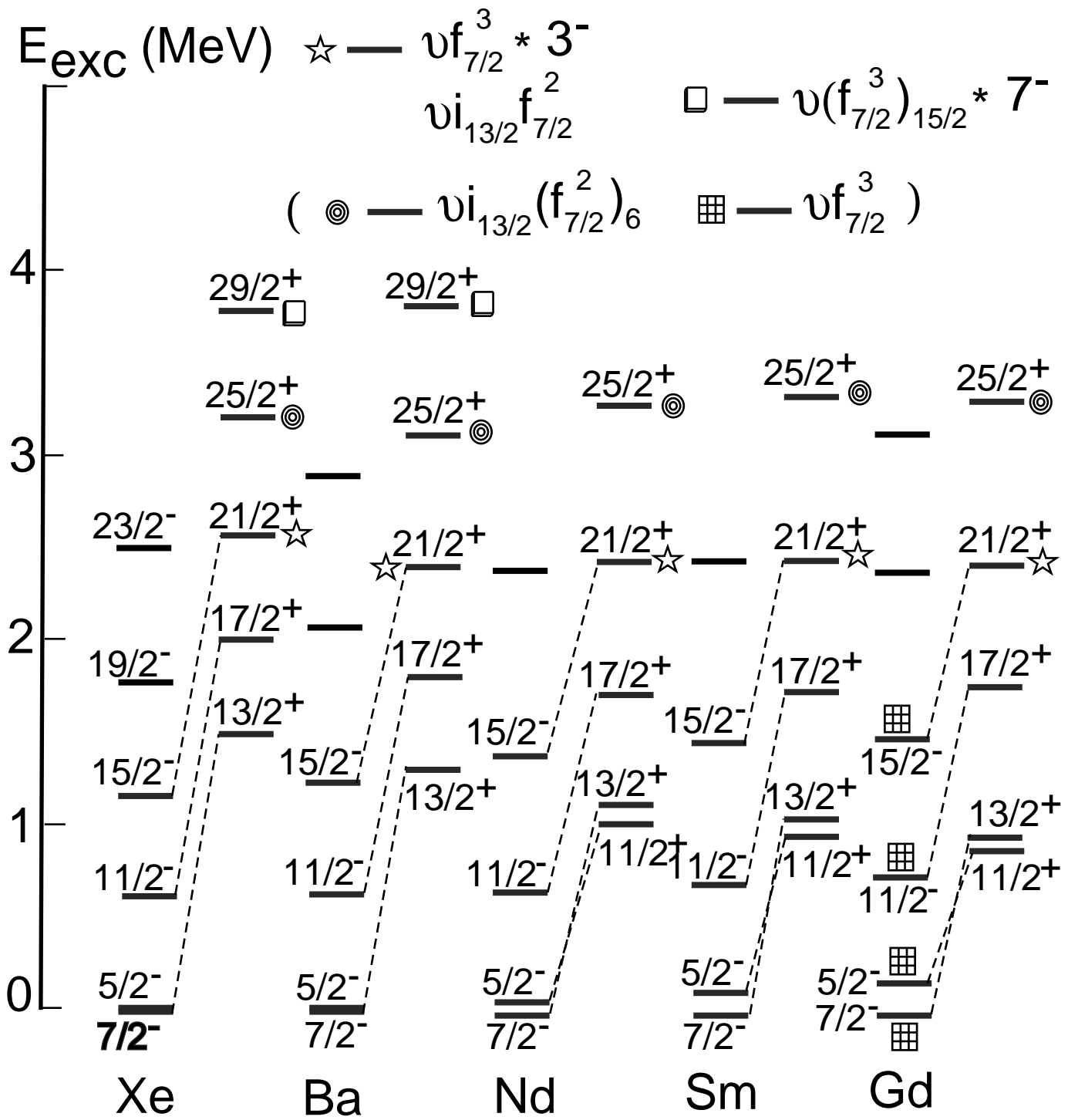
(5)

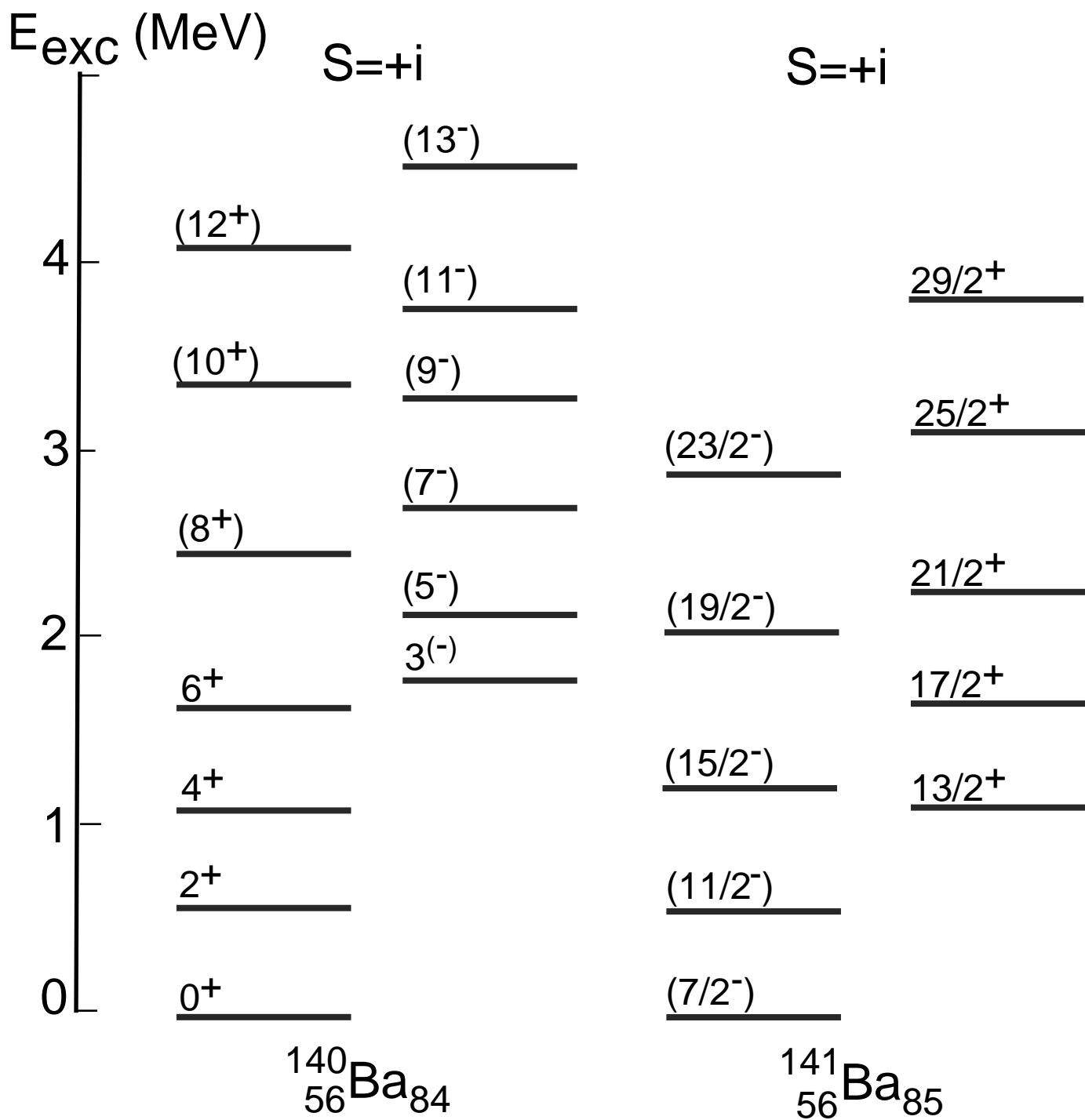
(6)



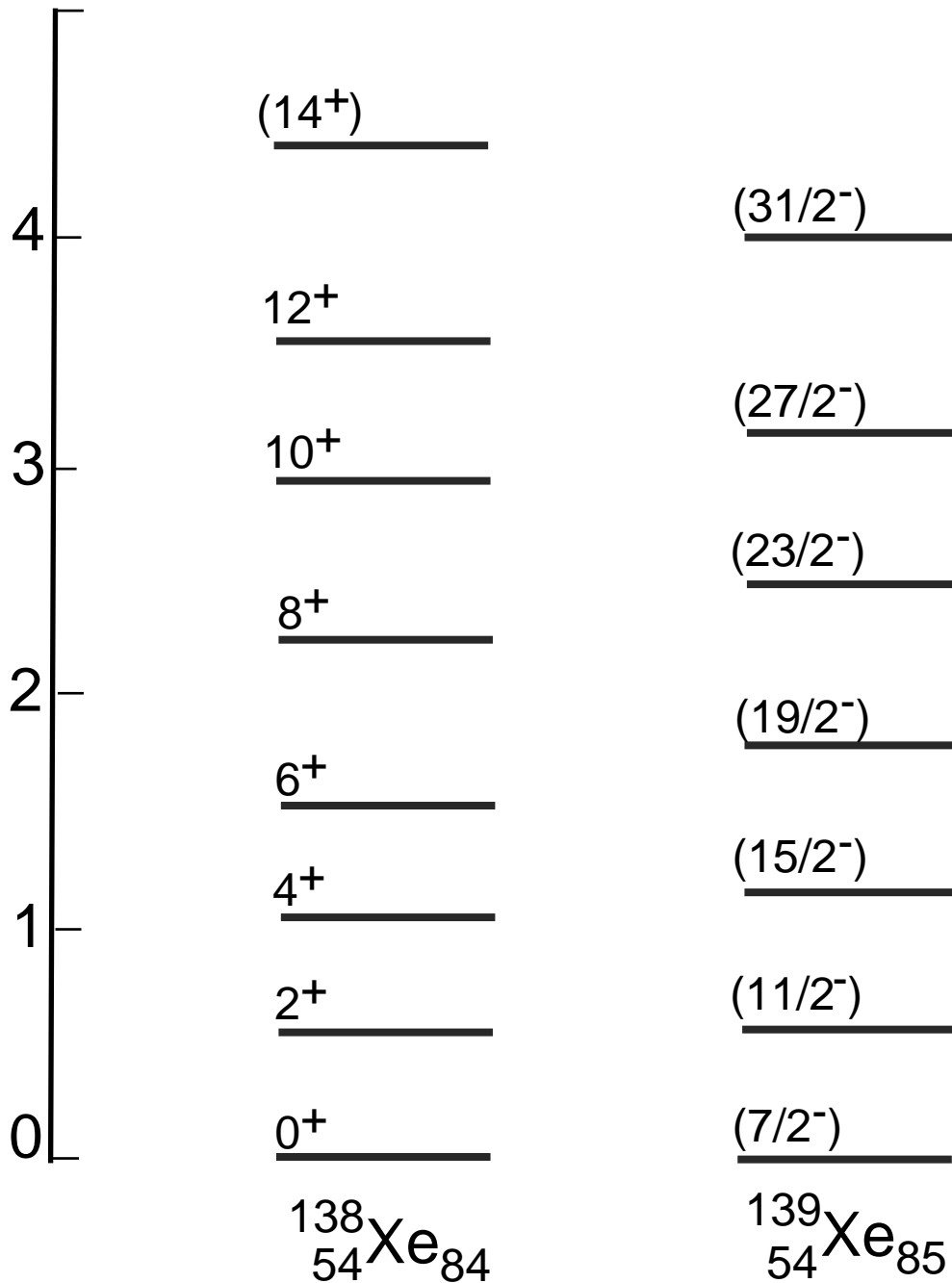


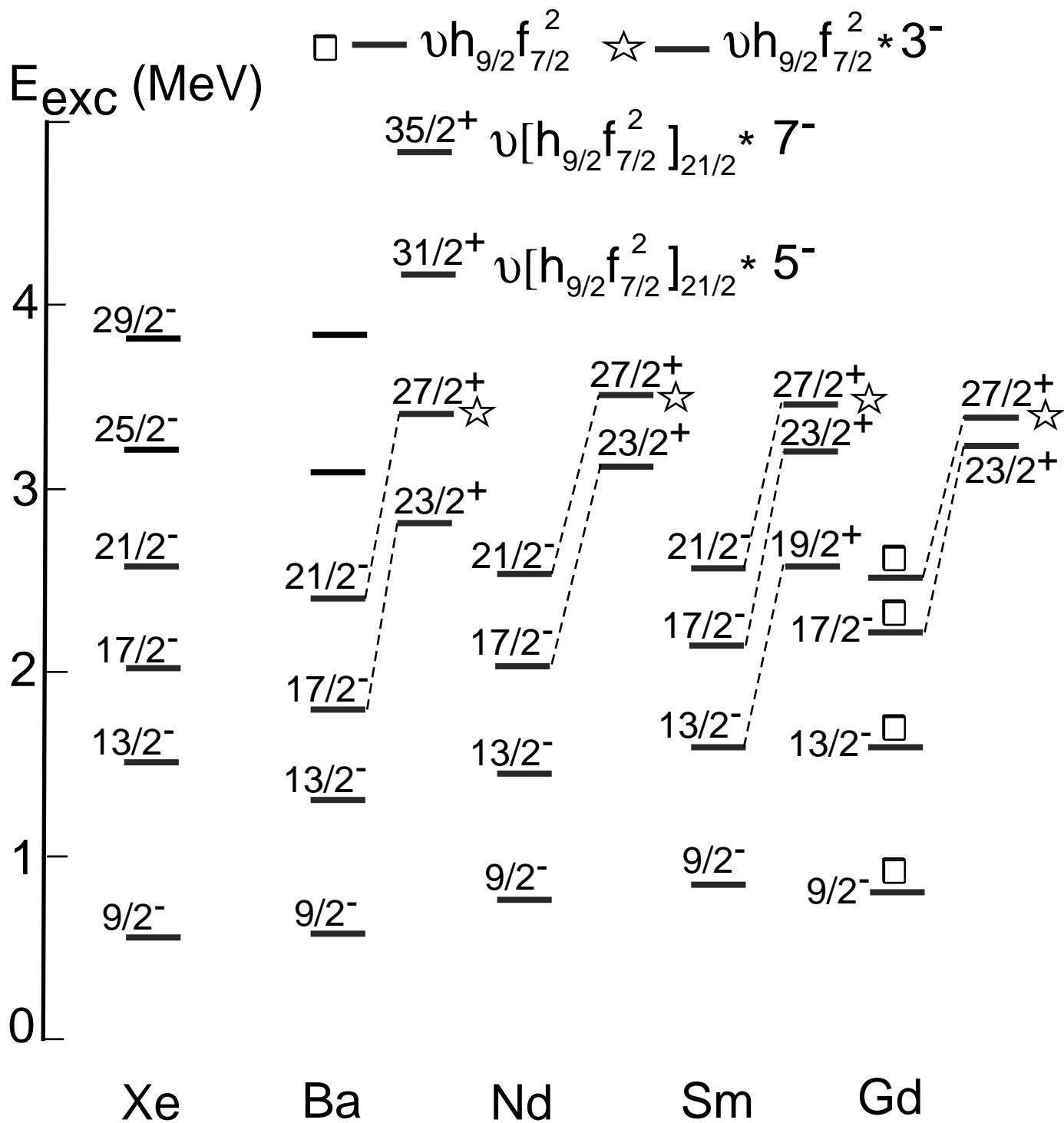






$E_{\text{exc}}$  (MeV)





$E_{exc}$  (MeV)

2.0

1.0

0.0

Te

Xe

Ba

Nd

Sm

Gd

$13/2^-$

$13/2^+$

$\nu(f_{7/2}^3) * 3^-$

$E(3^-, N=84) - E(13/2^+, N=85)$

